Clutter Non Gaussiano e controllo dei falsi allarmi

Pierfrancesco Lombardo

Tel: 06- 44585472 (interno 25-472)

Statistical modeling of radar clutter

- Empirically observed models (Rayleigh, Weibull, K, generalized K, log-normal, etc.)
- Extension of the Central Limit Theorem (CLT): the compound-Gaussian model
- Multidimensional models of random clutter vectors

The problem of radar clutter modeling

- In early studies the resolution capabilities of radar systems were relatively low, and the scattered return from clutter was thought to comprise a large number of scatterers
- From the Central Limit Theorem (CLT), Researchers in the field were led to conclude that the appropriate statistical model for clutter was the **Gaussian** model (i.e., the amplitude is **Rayleigh** distributed)

$$R = |Z| = \sqrt{Z_I^2 + Z_Q^2}$$

$$Z = Z_I + jZ_Q$$

$$p_R(r) = \frac{r}{\sigma^2} \exp\left(-\frac{r^2}{2\sigma^2} \right) u(r)$$

$$p_Z(z) = \frac{1}{2\pi\sigma^2} \exp\left(-\frac{|z|^2}{2\sigma^2} \right)$$

The problem of radar clutter modeling

- Presently, the resolution capabilities of radar systems have been improved
- For detection performance, the belief originally was that a higher resolution radar system would intercept less clutter than a lower resolution system, thereby increasing detection performance
- However, as resolution has increased, the statistics of the noise have no longer been observed to be Gaussian, and the detection performance has not improved directly
- The radar system is now plagued by target-like "spikes" that give rise to non-Gaussian observations
- These spikes are passed by the detector as targets at a much higher false alarm rate (FAR) than the system is designed to tolerate
- The reason for the poor performance can be traced to the fact that the traditional radar detector is designed to operate against Gaussian noise
- New clutter models and new detection strategies are required to reduce the effects of the spikes and to improve detection performance

Empirically observed models

- Empirical studies have produced several candidate models for spiky non-Gaussian clutter, the most popular being the Weibull distribution, the K distribution, and the log-normal distribution (two-parameters PDFs)

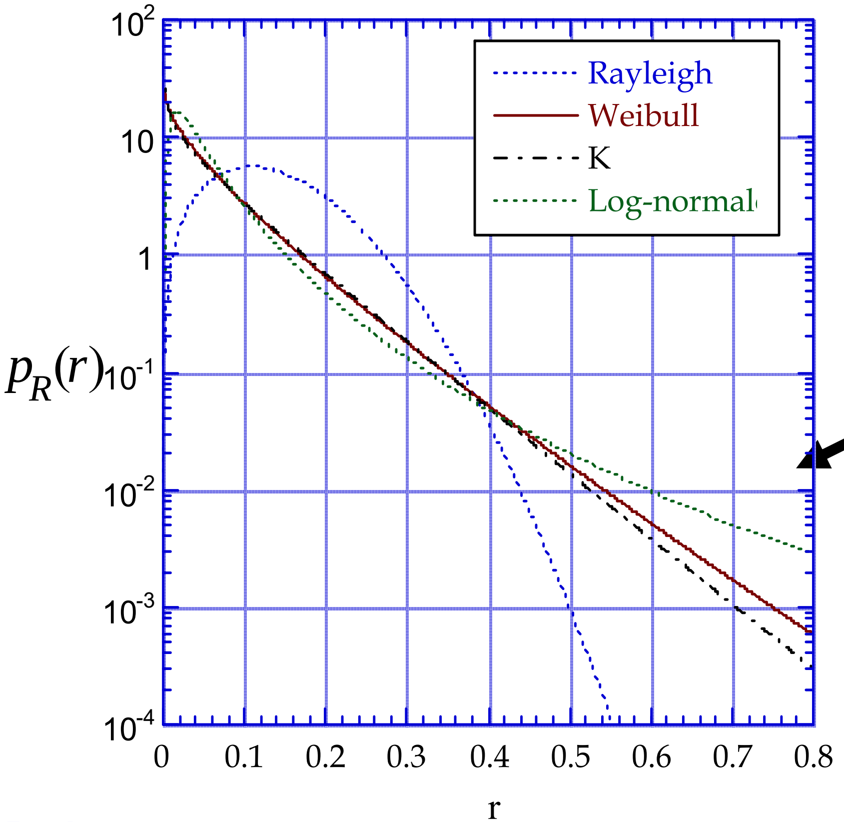

Expressions of the probability density functions (PDFs) and their moments are reported in Sect. 3.1

identical 1st and 2nd order moments (only the 2nd one for the Rayleigh PDF)

Weibull , K, and log-normal have heavier tails than Rayleigh

Clutter PDF (I)

AMPLITUDE PDF ANALYSIS

Log-normal distribution

θ scale parameter

δ shape parameter

PDF: $$p_Z(z) = \frac{\delta}{z\sqrt{2\pi}} \exp\left(-\frac{1}{2} (\vartheta + \delta \ln(z))^2 \right) u(z)$$

Moments: $$E\{Z^n\} = \exp\left[\frac{n}{\delta} \left(\frac{n}{2\delta} - \vartheta \right) \right]$$

Weibull distribution

b **scale parameter**

c **shape parameter**

PDF: $$p_Z(z) = \frac{c}{b} \left(\frac{z}{b} \right)^{c\text{-}1} \exp\left[-(z/b)^c \right] u(z)$$

Moments: $$E\left\{Z^n\right\} = b^n \Gamma(n/c + 1)$$

The compound-Gaussian model

- After studying the problem of sea clutter modeling, Trunk concluded that some types of non-Rayleigh sea clutter may be modeled as a **locally homogeneous Rayleigh process whose parameter (which represents the local clutter power in this case) is modulated due to the radar's large scale spatial sampling of the environment**
- The amplitude PDF (APDF) of such a model may be written as:

$$p_R(r)=\int_0^\infty \frac{r}{\tau}\, e^{-\frac{r^2}{2\tau}}\, p_\tau(\tau)\,d\tau$$

it was referred to as the **Rayleigh mixture** model (others called it the **compound-Gaussian** model)

- Jakeman and Pusey showed that a modification of the CLT to include random fluctuations of the number *N* of scatterers could give rise to the K distribution (for APDF):

$$Z=\frac{1}{\sqrt{\overline{N}}}\sum_{i=1}^{N} a_i e^{j\varphi_i} \xrightarrow{\overline{N}\to\infty} R=|Z|$$

2-D random walk

K distributed if *N* is a negative binomial r.v. (Gaussian distributed if *N* is deterministic, Poisson, or binomial)

$$\overline{N}=E\{N\},\ \{a_i\}\ i.i.d.,\ \{\varphi_i\}\ i.i.d.$$

The K model

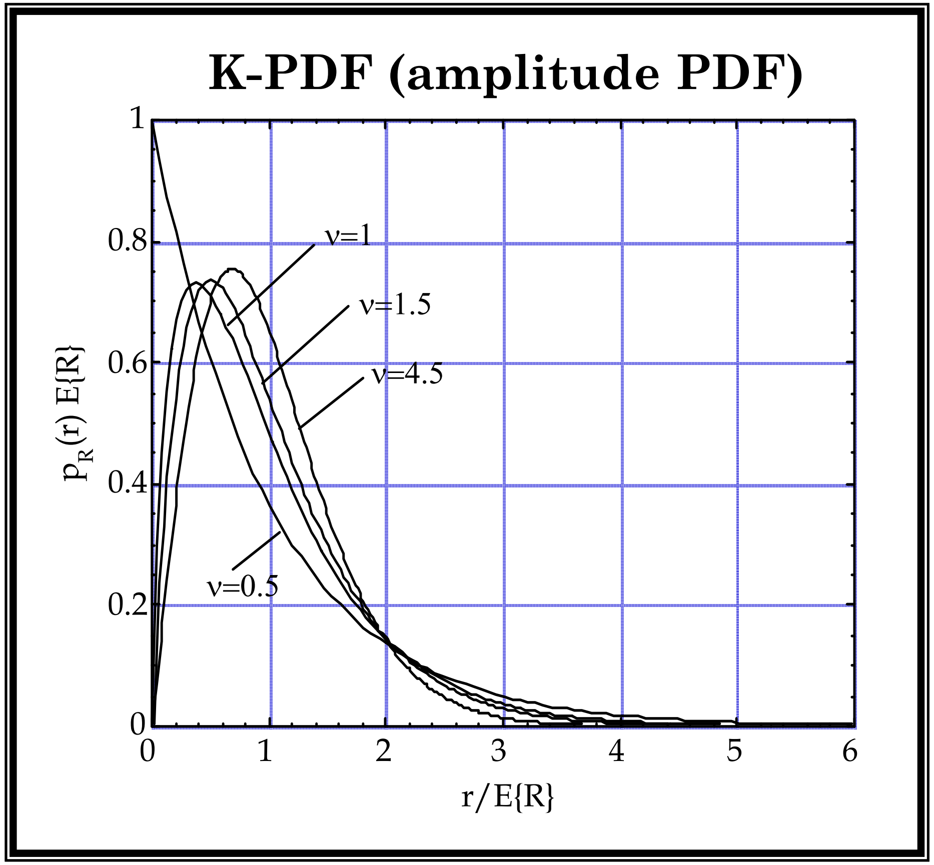

The K model is a special case of the compound-Gaussian model:

N = negative binomial r.v.

τ (local clutter power) = Gamma distributed

Amplitude R = K distributed

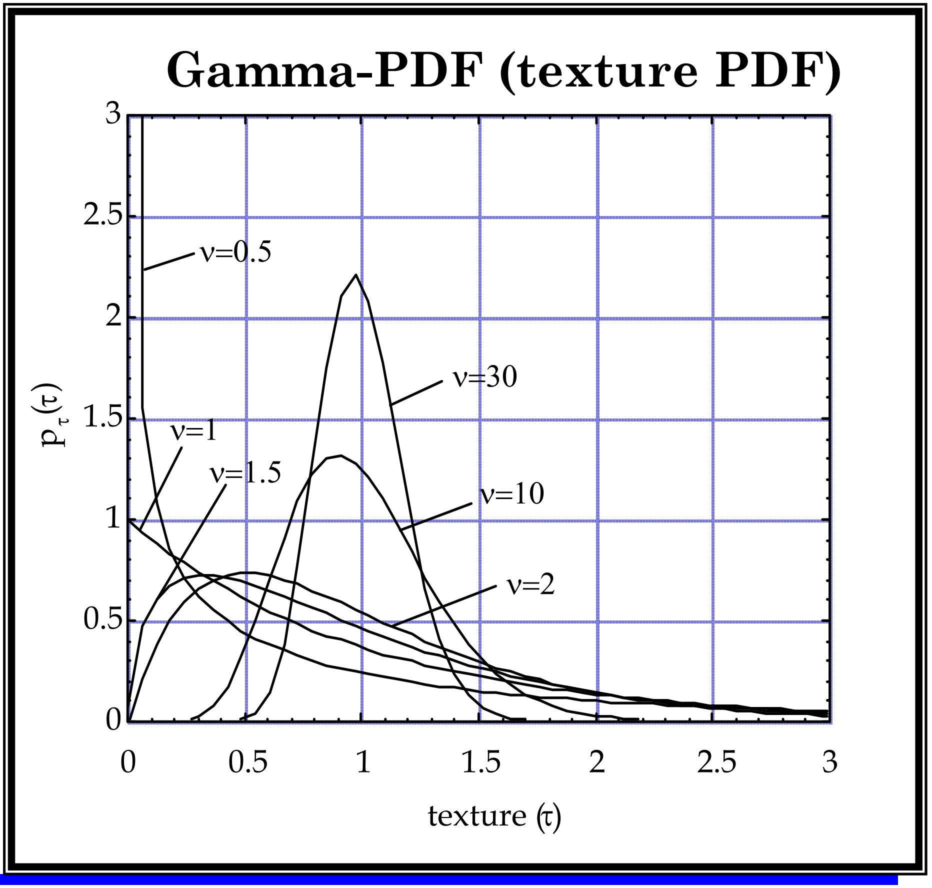

- The order parameter ν is a measure of clutter spikiness
- The clutter becomes spikier as ν decreases
- Gaussian clutter: $\nu \rightarrow \infty$

Clutter PDF (II)

AMPLITUDE PDF ANALYSIS

Rayleigh distribution

b **scale parameter**

PDF: $p_z(z)=\frac{2z}{b^2}\exp\left[-(z/b)^2\right]u(z)$

Moments: $E\{Z^n\}=b^n\Gamma(n/2+1)$

K-distribution

μ scale parameter

ν order parameter

PDF: $p_Z(z)=\frac{\sqrt{2\,\nu/\mu}}{\Gamma(\,\nu)2^{\nu-1}}\left(\sqrt{\frac{2\,\nu}{\mu}}z\right)^{\nu}K_{\nu-1}\left(\sqrt{\frac{2\,\nu}{\mu}}z\right)u(z)$

Moments: $E\left\{Z^n\right\}=\frac{(2\mu)^{n/2}\,\Gamma\left(\nu+n/2\right)\Gamma\left(n/2+1\right)}{\nu^{n/2}\,\Gamma(\,\nu)}$

Land clutter statistics

	1st order	2nd order
Time	Rayleigh Rice (Weibull, log-normal)	Gaussian Spectrum
Space	Weibull Log-normal	Independent clutter returns from different cells

First order statistics:
because of the large spatial variability of land clutter the statistics in space and time are different.
The homogeneity of sea allows to consider its spatial distribution equivalent to the temporal distribution. The same is not true for land clutter.

Spatial amplitude distribution

Weibull distribution

Weibull p.d.f. is in use to represent the spatial statistics of land clutter. Recently the MIT Lincoln Laboratory has proposed the Weibull model in consequence of extensive ground clutter measurement campaign.

The model consists of 27 combinations of terrain type and depression angle. For each combination the clutter model provides:

• the mean clutter strength $\sigma^0(f)$ as a function of radar frequency (VHF through X-band)

• the slope parameter α as a function of the radar spatial resolution over the range between 10^3 m^2 and 10^6 m^2..

Mean strength σ^0

- At all frequencies a significant trend of increasing strength with increasing depression angle can be seen.
- Strong dependence from depression angle is observed for continuous forest and desert/grassland.
- As general trend σ^0 shows the tendency to increase with increasing frequency
- Exceptions can be found looking at urban area, general rural and forest data, in which σ^0 shows a fairly constant value at L, S and X-band.
- There is an opposite trend for forest at relatively high depression angle (1° and 2°). We can see decreasing strength with increasing frequency. This is caused by the absorption characteristics of the foliage.

Slope Parameter α

•In general at low angles the distribution is very broad and differs substantially from Rayleigh (α=1).

•With increasing angle the spread decreases. For high angles the statistics tends to be very close to Rayleigh.

•The spread parameter is decreasing with increasing cell size. As the cell increases, the amount of scatterers within the cell increases and the variability from cell to cell decreases.

•Spread is dependent on the homogeneity of the surface. So it tends to be very high for urban areas while less spread occurs for example in forest because it is more homogeneous surface.

Weibull parameters

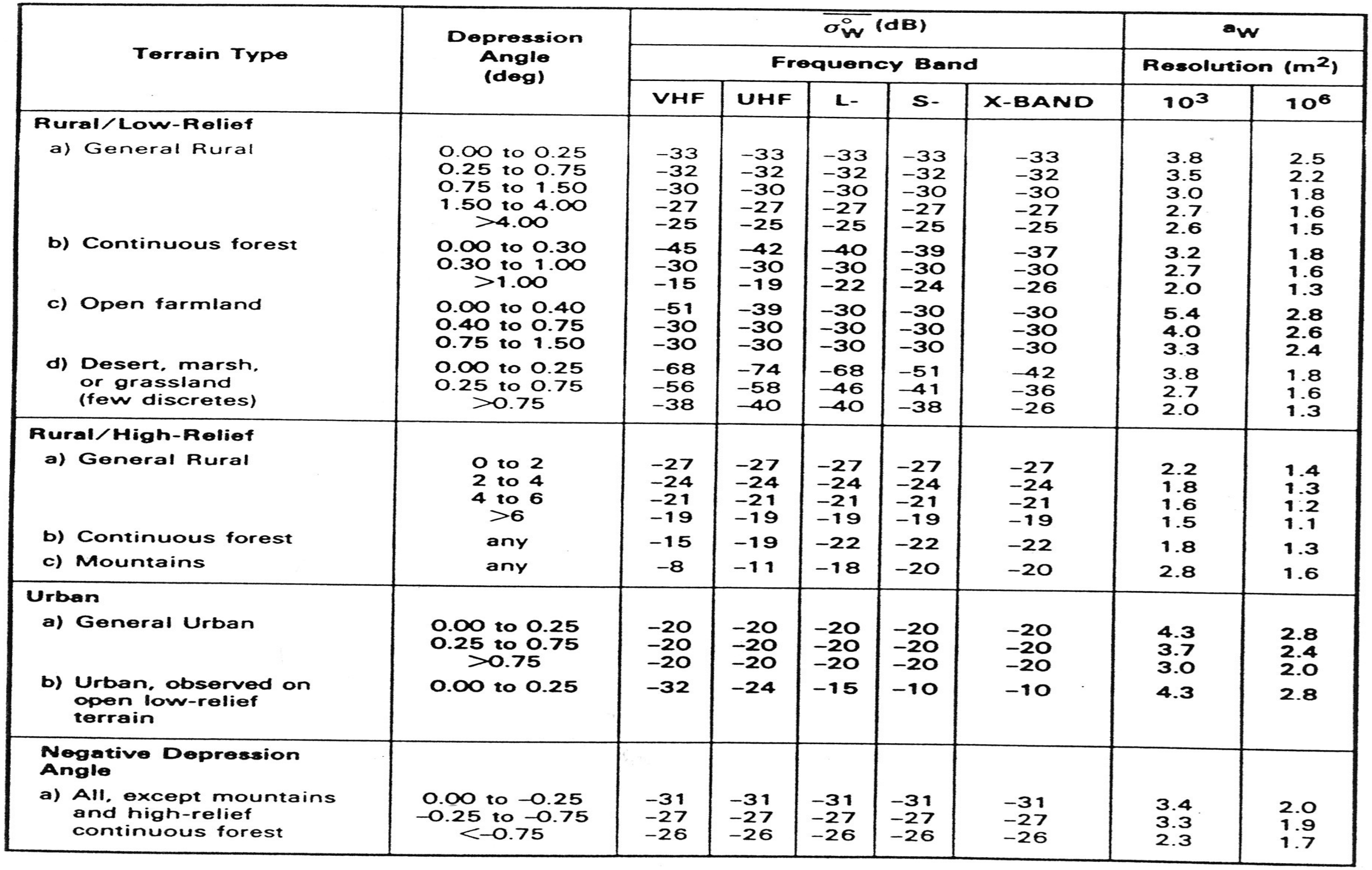

Terrain Type	Depression Angle (deg)	$\overline{\sigma^\circ_W}$ (dB)					a_W	
		Frequency Band					Resolution (m^2)	
		VHF	UHF	L-	S-	X-BAND	10^3	10^6
Rural/Low-Relief								
a) General Rural	0.00 to 0.25	−33	−33	−33	−33	−33	3.8	2.5
	0.25 to 0.75	−32	−32	−32	−32	−32	3.5	2.2
	0.75 to 1.50	−30	−30	−30	−30	−30	3.0	1.8
	1.50 to 4.00	−27	−27	−27	−27	−27	2.7	1.6
	>4.00	−25	−25	−25	−25	−25	2.6	1.5
b) Continuous forest	0.00 to 0.30	−45	−42	−40	−39	−37	3.2	1.8
	0.30 to 1.00	−30	−30	−30	−30	−30	2.7	1.6
	>1.00	−15	−19	−22	−24	−26	2.0	1.3
c) Open farmland	0.00 to 0.40	−51	−39	−30	−30	−30	5.4	2.8
	0.40 to 0.75	−30	−30	−30	−30	−30	4.0	2.6
	0.75 to 1.50	−30	−30	−30	−30	−30	3.3	2.4
d) Desert, marsh, or grassland (few discretes)	0.00 to 0.25	−68	−74	−68	−51	−42	3.8	1.8
	0.25 to 0.75	−56	−58	−46	−41	−36	2.7	1.6
	>0.75	−38	−40	−40	−38	−26	2.0	1.3
Rural/High-Relief								
a) General Rural	0 to 2	−27	−27	−27	−27	−27	2.2	1.4
	2 to 4	−24	−24	−24	−24	−24	1.8	1.3
	4 to 6	−21	−21	−21	−21	−21	1.6	1.2
	>6	−19	−19	−19	−19	−19	1.5	1.1
b) Continuous forest	any	−15	−19	−22	−22	−22	1.8	1.3
c) Mountains	any	−8	−11	−18	−20	−20	2.8	1.6
Urban								
a) General Urban	0.00 to 0.25	−20	−20	−20	−20	−20	4.3	2.8
	0.25 to 0.75	−20	−20	−20	−20	−20	3.7	2.4
	>0.75	−20	−20	−20	−20	−20	3.0	2.0
b) Urban, observed on open low-relief terrain	0.00 to 0.25	−32	−24	−15	−10	−10	4.3	2.8
Negative Depression Angle								
a) All, except mountains and high-relief continuous forest	0.00 to −0.25	−31	−31	−31	−31	−31	3.4	2.0
	−0.25 to −0.75	−27	−27	−27	−27	−27	3.3	1.9
	<−0.75	−26	−26	−26	−26	−26	2.3	1.7

Multifrequency Weibull parameters of ground clutter amplitude distributions.

Log-Normal distribution

Another distribution used to represent the cell by cell variation of land clutter is the Log-Normal.

Terrain	**Frequency Band**	**Grazing Angle (°)**	σ_p
Discrete	S	Low	3.916
Distributed	S	Low	1.380
Various	UHF-K_a	10-70	0.728-2.584

Ground clutter data analysis

<u>Windblown trees</u> **These data are Gaussian**

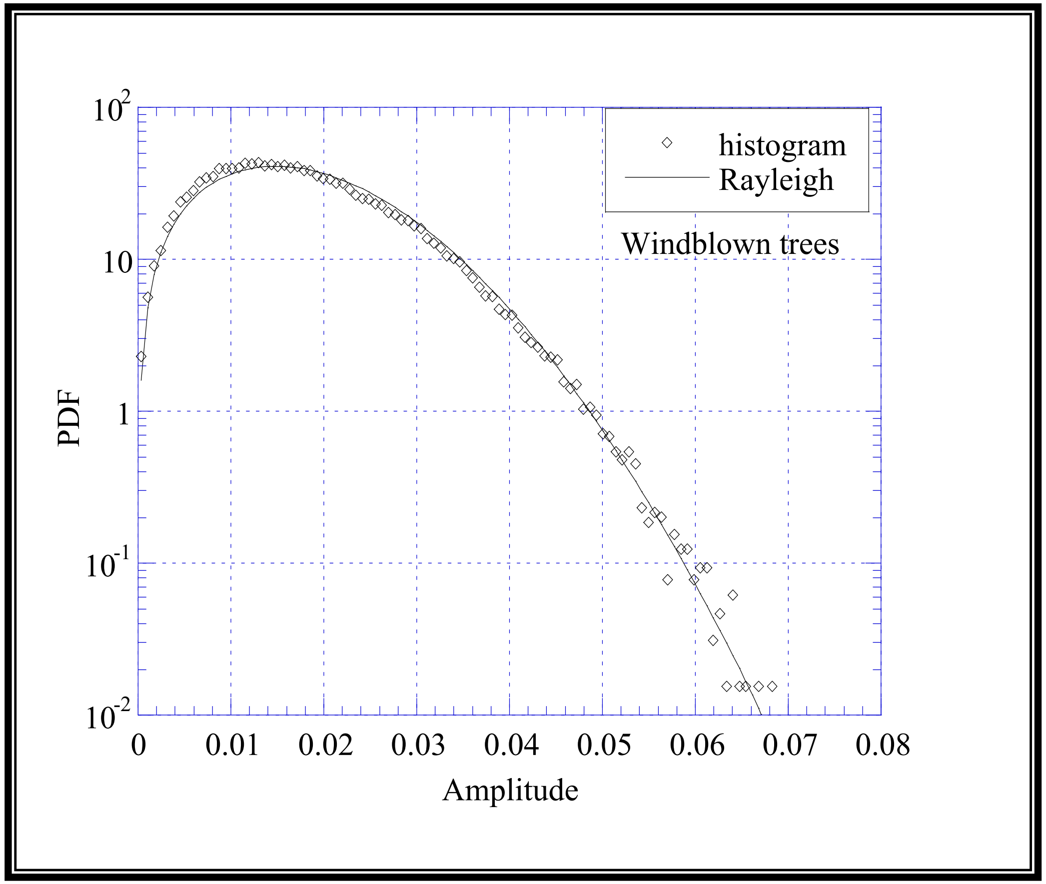

Ground clutter data analysis

Amplitude PDF analysis:

(use method of moments):

normalized moments defined as

$$m_Z(n) \overset{\Delta}{=} \frac{E\{Z^n\}}{E^n\{Z\}}$$

Range interval	K distribution		Log-normal distr.		Weibull distr.	
	ν	μ	δ	ϑ	c	b
1st HH	3.68E-2	8.46E-5	0.633	4.33	0.39	1.01E-3
1st VV	4.43E-2	1.25E-4	0.655	4.24	0.41	1.56E-3
2nd HH	5.12E-2	1.58E-4	0.673	4.19	0.43	2.09E-3
2nd VV	4.48E-2	3.02E-4	0.656	3.96	0.41	2.46E-3
3rd HH	5.32E-2	1.85E-4	0.68	4.16	0.43	2.37E-3
3rd VV	4.55E-2	3.71E-4	0.658	3.89	0.41	2.78E-3
4th HH	8.48E-2	7.49E-5	0.749	4.63	0.50	2.54E-3
4th VV	7.07E-2	1.44E-4	0.720	4.32	0.47	2.91E-3

Table 3 - Scale and shape estimated parameters for the K, LN and Weibull P

Ground clutter data analysis

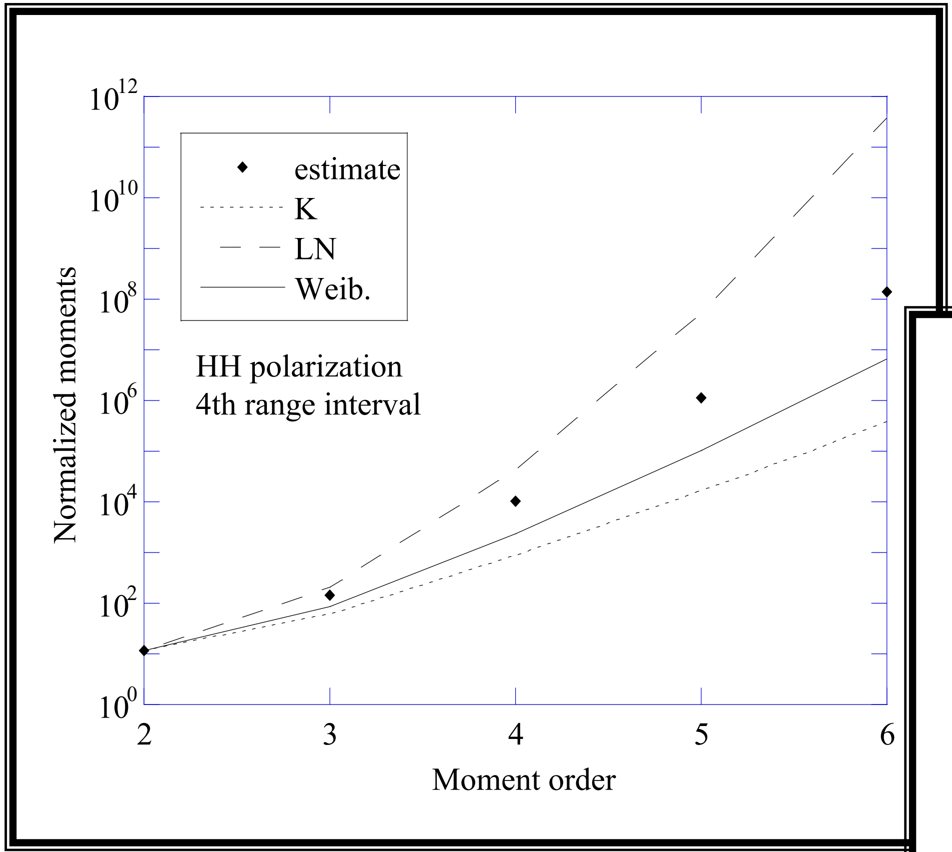

1st and 2nd range intervals:
the Weibull distribution provides the best fitting

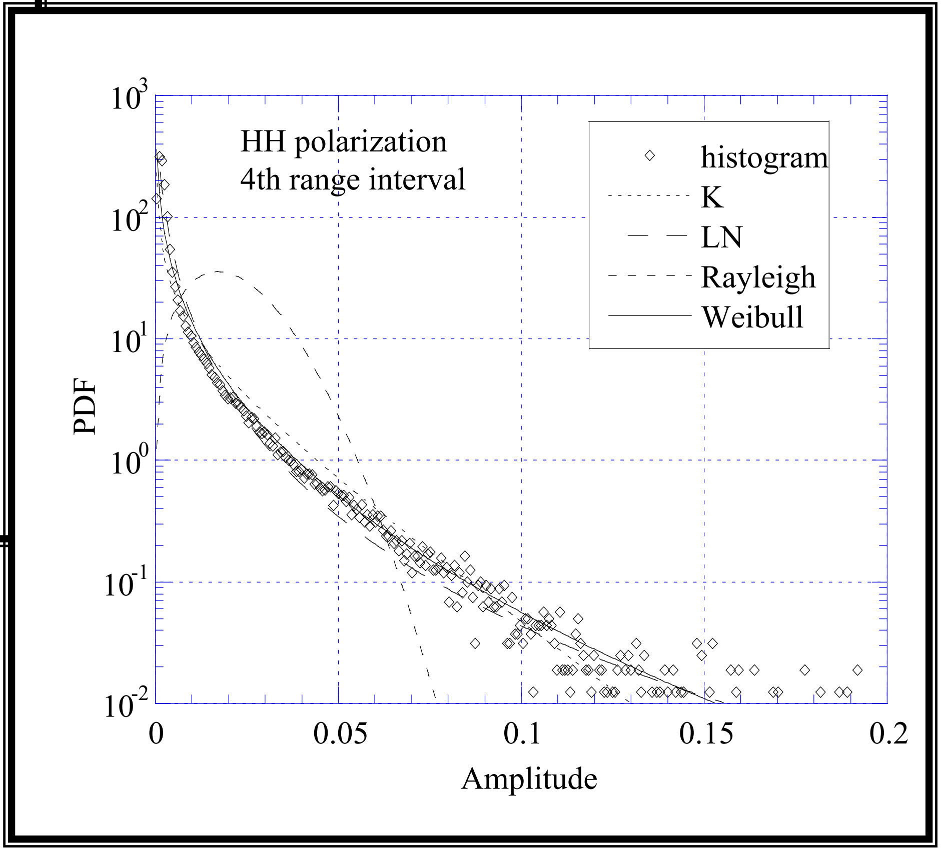

3rd and 4th range intervals:
the data show a behaviour intermediate between Weibull and log-normal

Temporal amplitude distribution

Recent analysis of experimental data has shown that the temporal statistics of ground clutter are best modeled by a Ricean distribution which sometimes degenerates into a Rayleigh distribution.

The Ricean model has some physical justification.

It is equivalent to consider the ground clutter as a combination of two components:

- Distributed Rayleigh-fluctuating clutter (or diffuse component)
- Discrete steady clutter, due for example to buildings or other large structures (coherent component).

Temporal amplitude distribution

A convenient parameter used for classification of clutter statistics is:

$$\beta = \frac{<V>^2}{<V^2>}$$

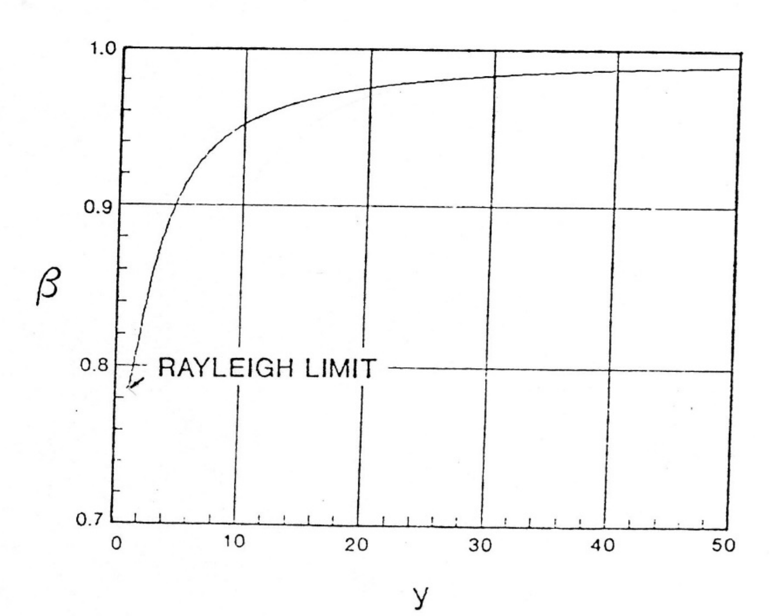

Parameter β as a function of y.

For the Rayleigh case β [illegible]

As the coherent component increases with respect to the diffuse component β approaches unity.

Experimental validation: sea clutter data

- Amplitude analysis of HH, VV, HV, and VH data
- Validation of the compound-Gaussian model by means of speckle and texture analyses

Sea clutter data recorded at McMaster University

IPIX radar parameters and sea state

Transmitter
- frequency agility (16 frequencies, X-band)
- H and V polarizations; switchable pulse-to-pulse
- pulse width 200 ns (range resolution 30 m), PRF=2KHz

Receiver
- coherent receiver
- 2 linear receivers; H or V on each receiver

Antenna
- parabolic dish
- pencil beam (beamwidth 0.9°)
- grazing angle 0.645°, azimuth fixed at 79.753°

Sea state condition during the trial of November 12, 1993
- sea state 3 (Beaufort scale)
- wind speed 22 km /h
- wind direction 40°
- significant wave height 1.42 m

Source: Defence Research Establishment Ottawa, courtesy Dr. A. Drosopoulos, Prof. S. Haykin

Sea clutter data analysis

The spikes have different behavior in the two like-polarizations (HH and VV)

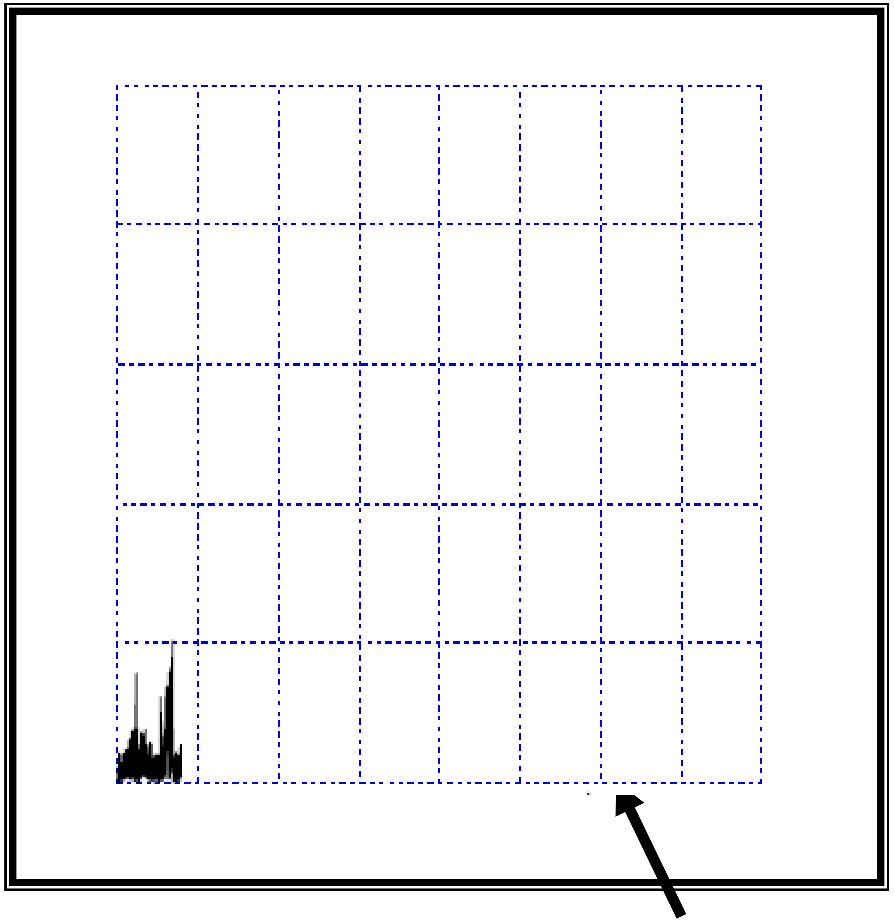

The dominant spikes on the HH record persist for about 1-2 s.

The vertically polarized returns appear to be a bit broader but less spiky

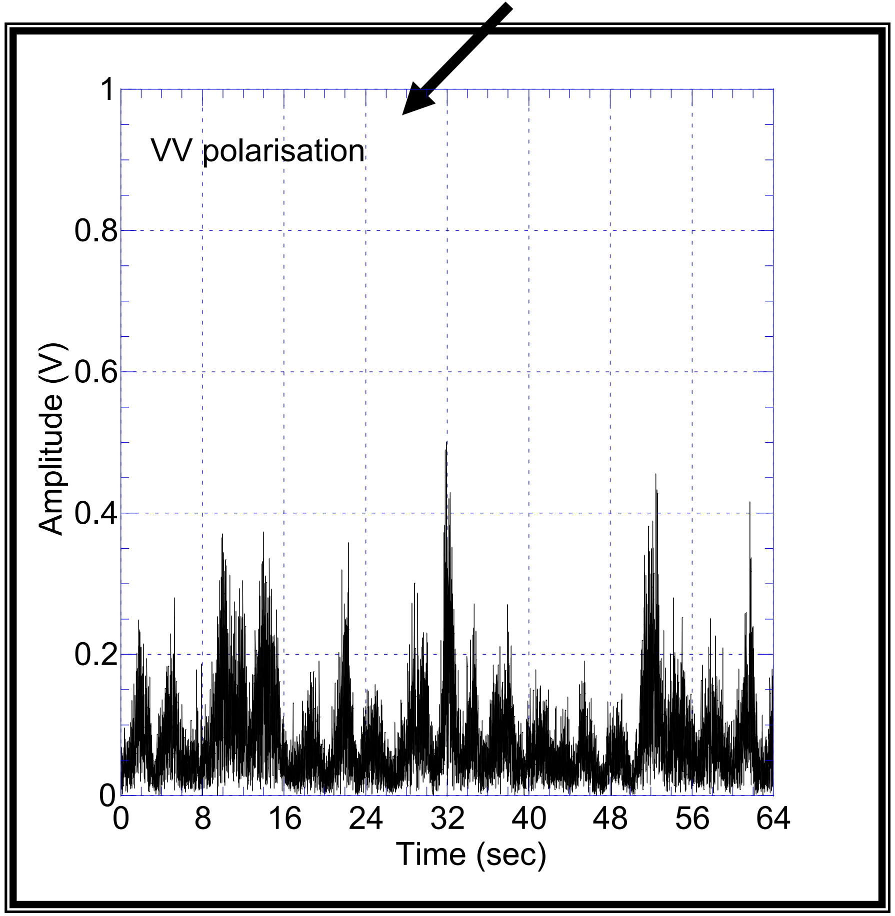

Sea clutter data analysis (I)

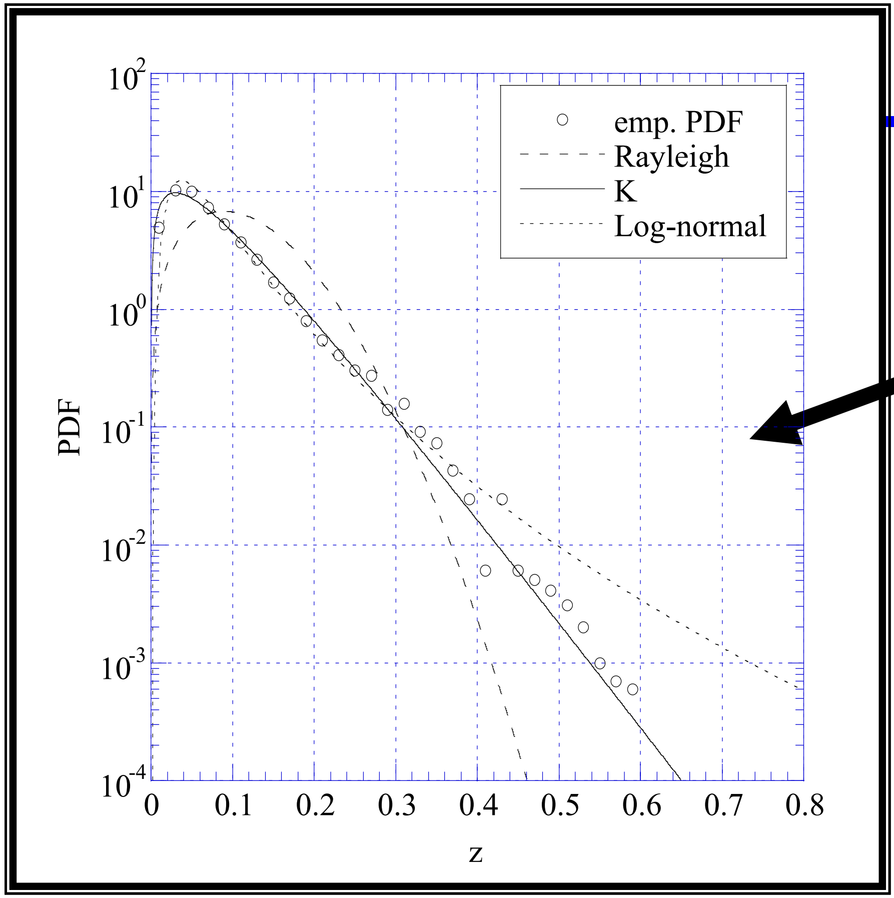

AMPLITUDE HISTOGRAMS (empirical PDF)

VV polarized data
best fitting: K distribution

The PDFs parameters have been estimated by the Method of Moments (MoM)

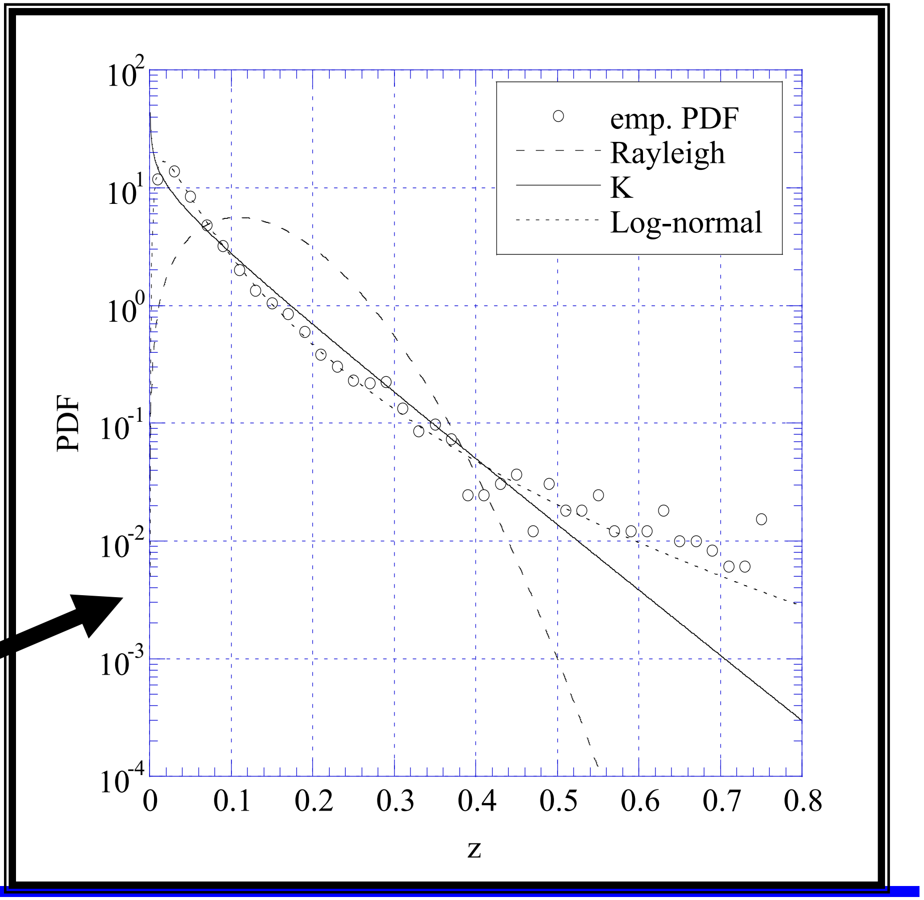

HH polarized data
best fitting: LN distribution

Sea clutter data analysis (II)

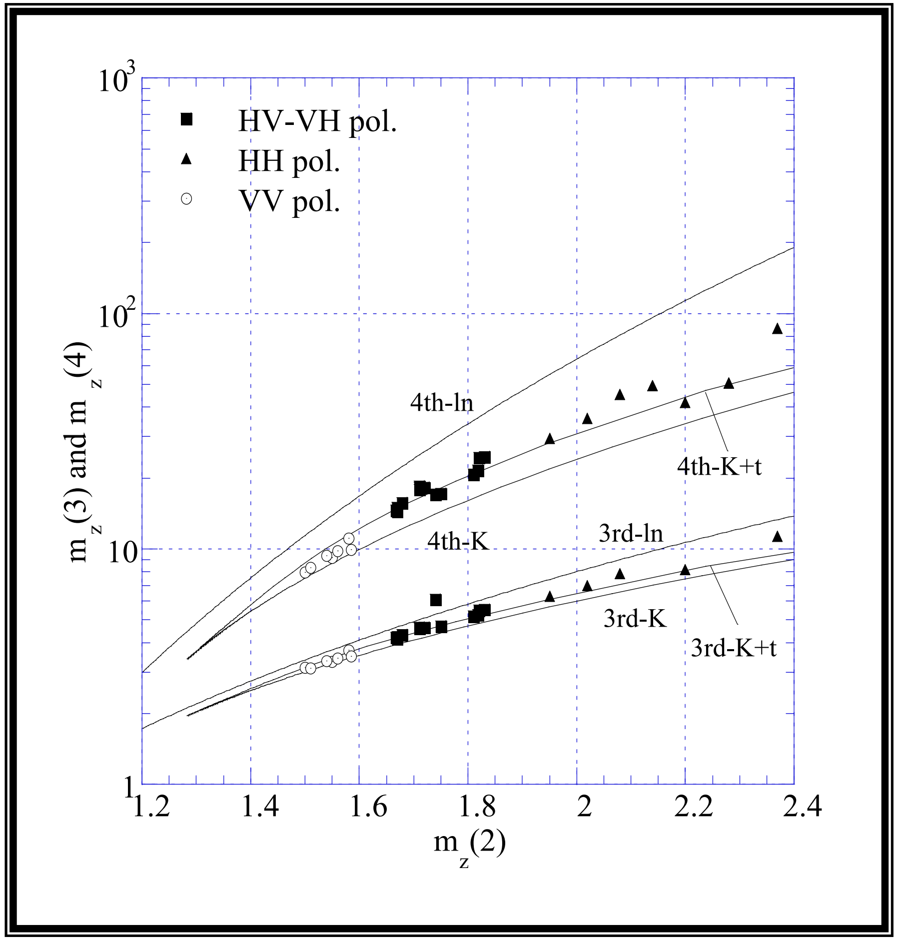

<u>For each polarization</u>: data from 7 range cells have been processed

- **<u>HH data</u>: behavior intermediate between K and LN distributions**
- **<u>VV data</u>: good agreement with the K model**
- **<u>HV-VH data</u>: estimated moments are very close to the theoretical moments of the K+thermal noise (K+t) model with *CNR=3 dB***

Sea clutter data analysis (III)

Validation of the K model

$$z[n]=\sqrt{\tau[n]}\,x[n]$$

texture **speckle**

The K distribution is a particular case of the more general compound-Gaussian model

- ✓ **The <u>texture</u>, associated with the bunching of scatterers, has a correlation time on the order of seconds**
- ✓ **The speckle has a correlation time on the order of 10 ms**

K distribution

<u>Speckle</u>: complex Gaussian distributed (the amplitude is Rayleigh distributed)

<u>Texture</u>: Gamma distributed

Sea clutter data analysis (IV)

Texture analysis: VV polarization

The texture has been isolated by averaging the modulus squared data over a window of 32 ms, to remove the speckle effect

$$\hat{\tau}[n]=\frac{1}{N}\sum_{k=n-N/2}^{n+N/2-1}\left|z[k]\right|^2$$

The texture data fit well a Gamma distribution

validation of the K-model for the VV data

$$p_\tau(\tau)=\frac{1}{\Gamma(\nu)}\left(\frac{\nu}{\mu}\right)^\nu \tau^{\nu-1}e^{-\frac{\nu}{\mu}\tau}u(\tau)$$

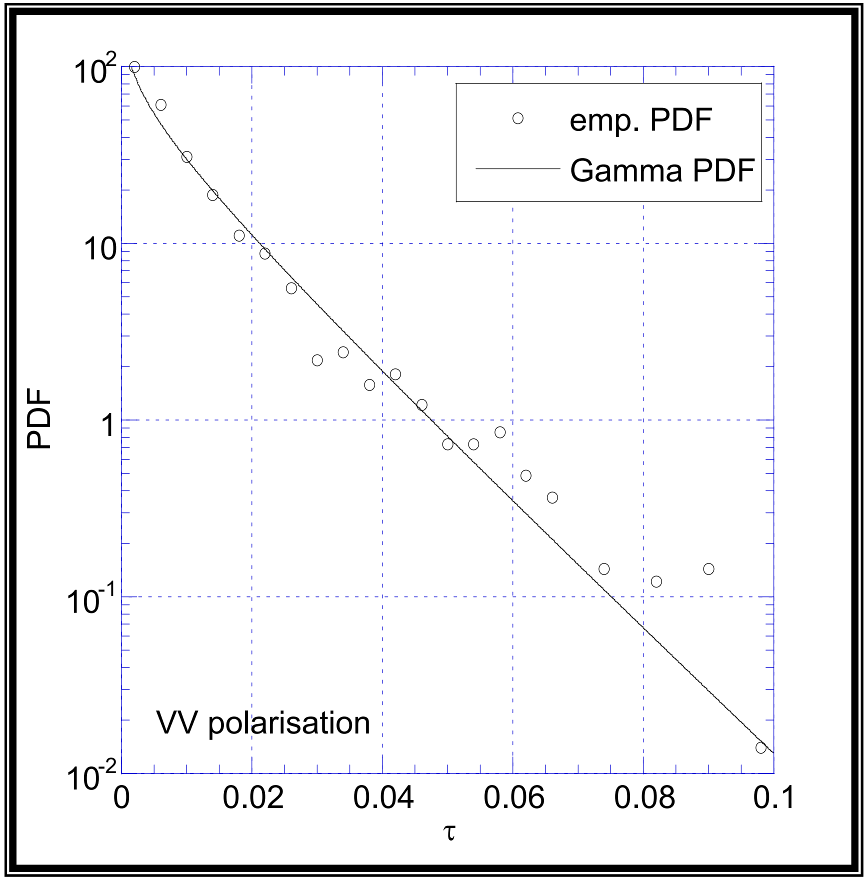

Sea clutter data analysis (V)

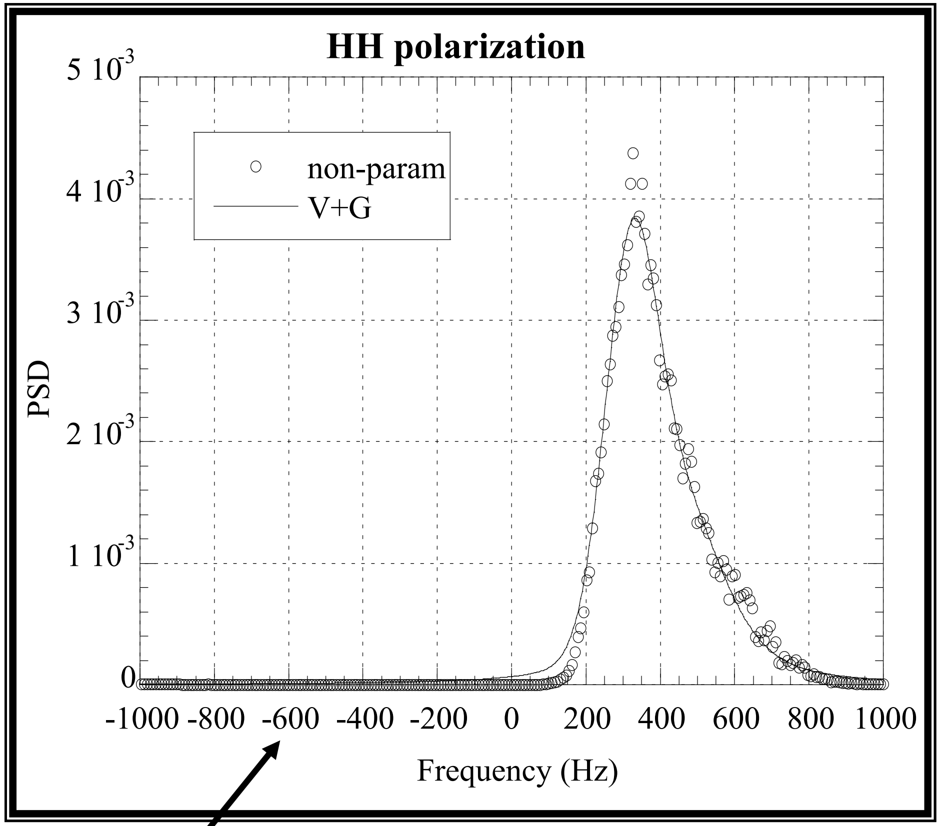

The spectrum is the sum of two basis functions: the Gaussian, the Lorentzian, and the Voigtian, with different Doppler peaks

non-par: modified periodogram
Gauss and Voigtian basis functions

High peak (Voigtian): 450 Hz
Low peak (Gaussian): 320 Hz

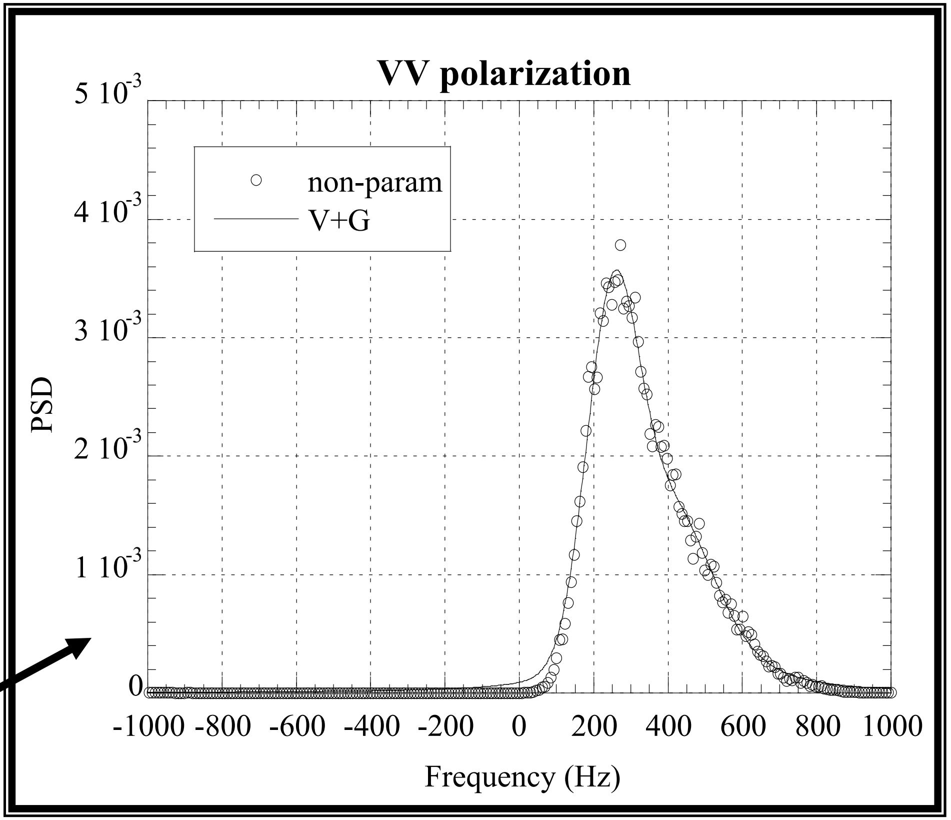

High peak (Voigtian): 410 Hz
Low peak: (Gaussian): 250 Hz

Summary of clutter PDF and moments

- Rayleigh pdf $p_x(x)=\frac{2x}{\mu}e^{-\frac{x^2}{\mu}}$ $x\geq 0$ $\left\langle x^n\right\rangle=\mu^{n/2}\Gamma(1+n/2)$

- Weibull pdf $p_x(x)=\frac{\alpha}{\beta}\left(\frac{x}{\beta}\right)^{\alpha-1}e^{-\left(\frac{x}{\beta}\right)^{\alpha}}$ $x\geq 0$ $\left\langle x^n\right\rangle=\beta^n\Gamma(1+n/\alpha)$

- Log-normal pdf $p_x(x)=\frac{1}{\sqrt{2\pi}\sigma x}e^{-\frac{(\ln x-\ln m)^2}{2\sigma^2}}$ $x>0$ $\left\langle x^n\right\rangle=m^n e^{n^2\sigma^2/2}$

- Chi-square (Gamma) pdf $p_x(x)=\frac{2}{\Gamma(\nu)}\left(\frac{\nu}{\mu}\right)^{\nu}x^{2\nu-1}e^{-\frac{\nu}{\mu}x^2}$ $x\geq 0$ $\left\langle x^n\right\rangle=\mu^{n/2}\frac{\Gamma(\nu+n/2)}{\nu^{n/2}\Gamma(\nu)}$

- K-pdf $p_x(x)=\frac{4}{\Gamma(\nu)}\left(\frac{\nu}{\mu}\right)^{\frac{\nu+1}{2}}x^{\nu}K_{\nu-1}\left(2\sqrt{\frac{\nu}{\mu}}x\right)$ $x\geq 0$ $\left\langle x^n\right\rangle=\mu^{n/2}\frac{\Gamma(\nu+n/2)}{\nu^{n/2}\Gamma(\nu)}\Gamma(1+n/2)$

Impact of PDF on single pulse CFAR detection

- **Constant False Alarm Rate (CFAR)** property is most important for radar systems, to avoid overload of the processors
- Clutter PDF has a significant impact on the one the CFAR property even in very simple single pulse radar systems
- Impact of non-Gaussianity on CFAR characteristic is shown in the following

Impact of PDF on performance: CFAR (I)

Consider samples of K-distributed clutter:
EXAMPLE of NON-GAUSSIAN

$$\mathbf{x}_k = \sqrt{\tau_k} \cdot \mathbf{g}_k$$

$$p_{\tau_k}(\tau_k) = \frac{1}{\Gamma(\nu)}\left(\frac{\nu}{\mu}\right)^{\nu} \tau_k^{\,\nu-1} \exp\left(-\frac{\nu}{\mu}\tau_k\right) \qquad \tau > 0$$

$$p_{I_{k,m}}(I_{k,m}) = \frac{2}{\Gamma(\nu)}\left(\frac{\nu}{\mu}\right)^{\frac{1+\nu}{2}} I_{k,m}^{\frac{\nu-1}{2}} K_{\nu-1}\left(2\sqrt{\frac{\nu}{\mu} I_{k,m}}\right)$$

Assume single-pulse detection using a **CA-CFAR** scheme (*z*=*I*)

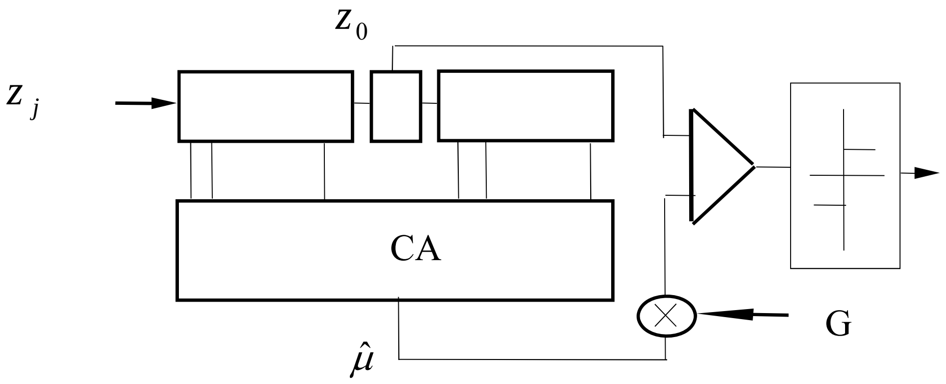

$$\boxed{z_0 > G \times \hat{\mu} = G \times \frac{1}{N}\sum_{j=1}^{N} z_j}$$

Impact of PDF on performance: CFAR (II)

The **probability of false alarm (P_{fa})** can be evaluated as:

$$P_{fa} = \Pr ob\left\{z_0 > G \cdot \hat{\mu} \;/\; H_0\right\} = \int_0^{\infty}\int_{G\hat{\mu}}^{\infty} p_Z(z_0)\, p_{\hat{\mu}}(\hat{\mu})\, dz_0\, d\hat{\mu}$$

$$P_{fa} = \int_0^{\infty} p_{\hat{\mu}}(\hat{\mu}) \int_{G\hat{\mu}}^{\infty} \int_0^{\infty} p(z_0 / \tau)\, p_\tau(\tau) d\tau\, d\, z_0\, d\hat{\mu}$$

If we replace the exact PDF $p_{\hat{\mu}}(\hat{\mu})$ with a Gamma PDF with the same mean value μ and order parameter ν_0, obtained by matching the Contrast of Amplitude of the two PDFs.

$$\boxed{P_{fa} = \sum_{i=1}^{L} \frac{\Gamma(L+\nu_0-i)}{(L-i)!\Gamma(\nu_0)} \frac{\Gamma(\nu+\nu_0)}{\Gamma(\nu)} \left(\frac{\nu}{\nu_0} GL\right)^{\nu} U\left(\nu+\nu_0, \nu-L+i+1, \frac{\nu}{\nu_0} GL\right)}$$

where U(·) is the Hypergeometric-U function and *L* is the number of degrees of freedom

Impact of PDF on performance: CFAR (III)

P_{fa} for single-pulse detection against K-distributed clutter

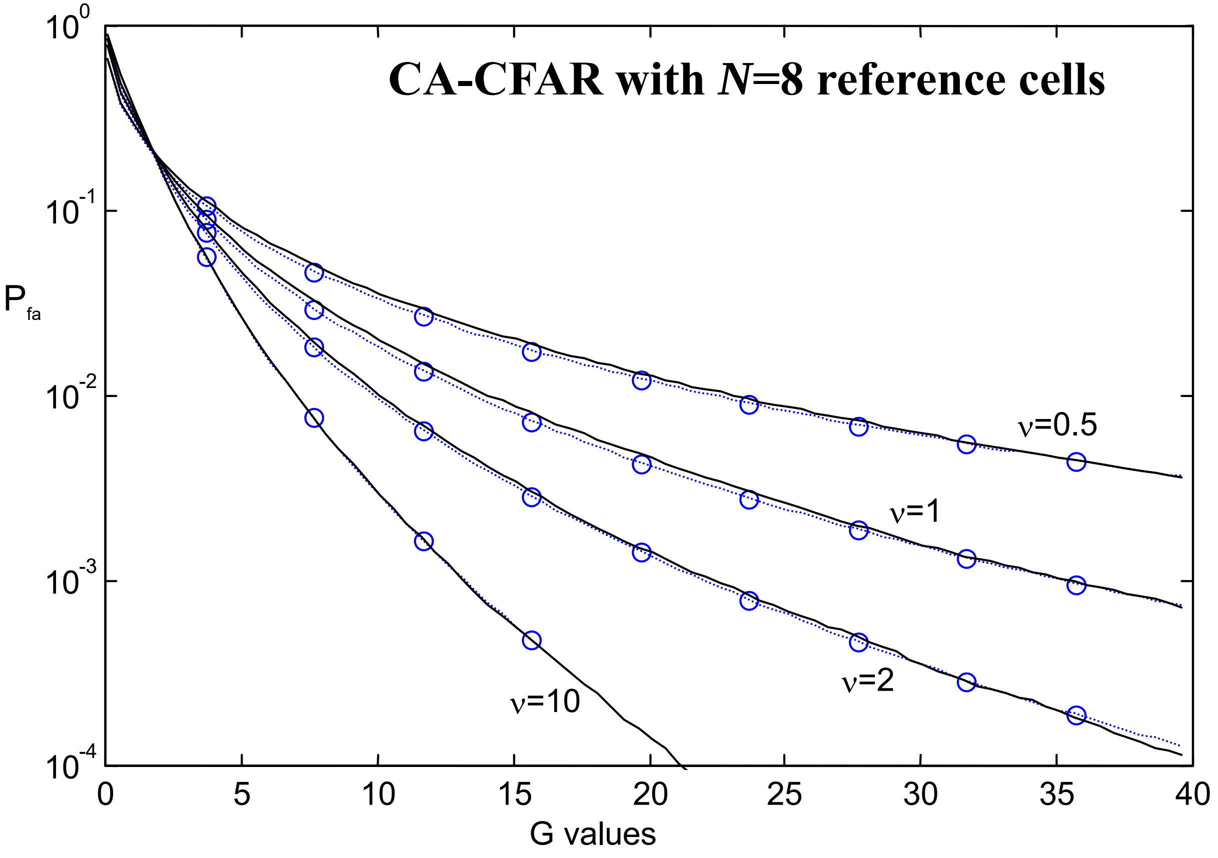

P_{fa} is largely affected by non-gaussianity

Comparison of analytical performance and simulated curves (10^6 trials)

Impact of PDF on performance: CFAR (IV)

P_{fa} for non-coherent detection (L=32 integrated pulses) against K-distributed clutter

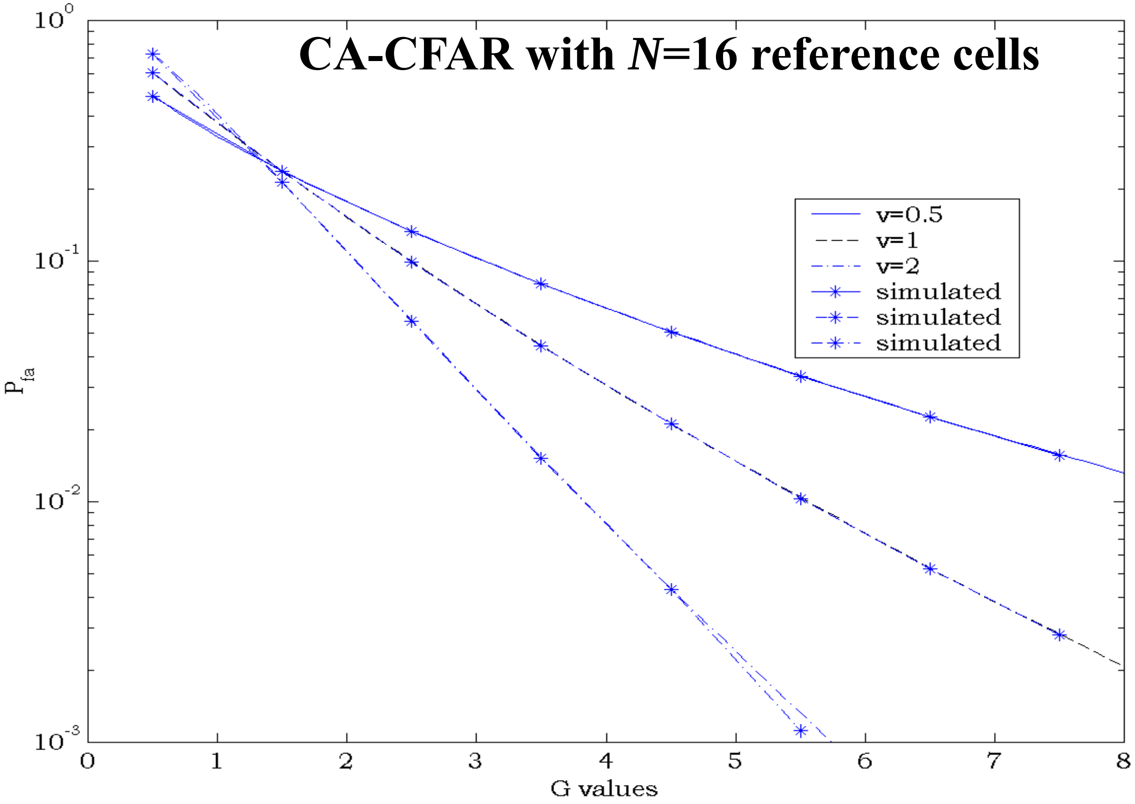

Comparison of analytical performance and simulated curves (10^6 trials)

Impact of PDF on performance: CFAR (V)

P_{fa} for single pulse detection CA-CFAR against Weibull and Log-normal Clutter

CA-CFAR with *N*=8 reference cells

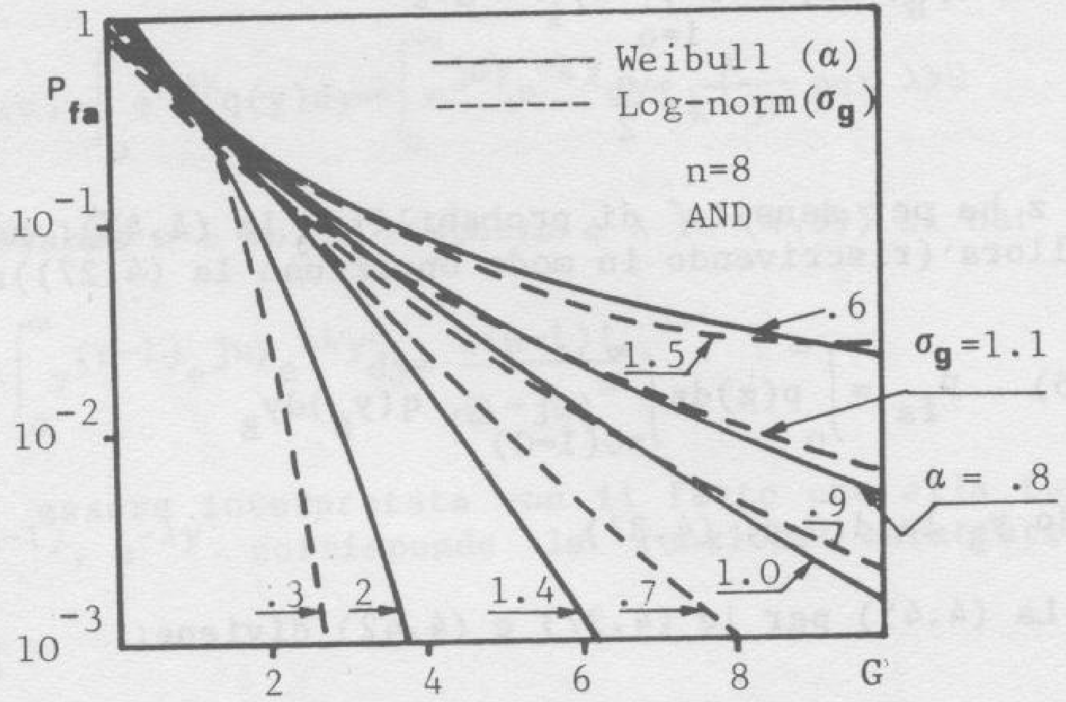

Fig.4.29 - Curve di falso allarme per un autogate tipo AND [28].

From: G. Picardi “Elaborazione del segnale radar”

Impact of PDF on performance: CFAR (VI)

P_{fa} for single pulse detection GO-CFAR against Weibull and Log-normal Clutter

GO-CFAR with *N*=8 reference cells

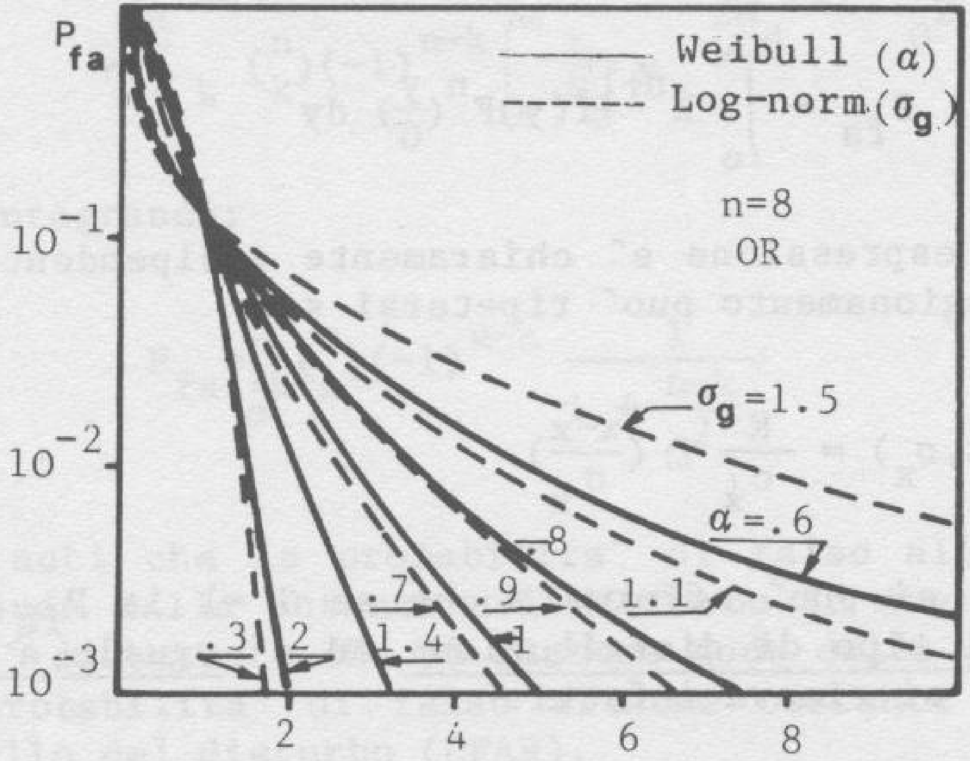

4.26 - Curve di falso allarme per un autogate tipo OR.

From: G. Picardi “Elaborazione del segnale radar”

Impact of PDF on performance: CFAR (VI)

Detection loss for single pulse detection GO-CFAR against Weibull (____) and Log-normal (- - - -) Clutter

$$\gamma_W = \frac{P_{fa}(\alpha)}{P_{fa\_desiderata}}\Bigg|_{\substack{G\,scelto\,per\,avere\,P_{fa\_desiderata}\\ contro\,clutter\,Gaussiano}}$$

$$\gamma_{LN} = \frac{P_{fa}(\sigma_g)}{P_{fa\_desiderata}}\Bigg|_{\substack{G\,scelto\,per\,avere\,P_{fa\_desiderata}\\ contro\,clutter\,Gaussiano}}$$

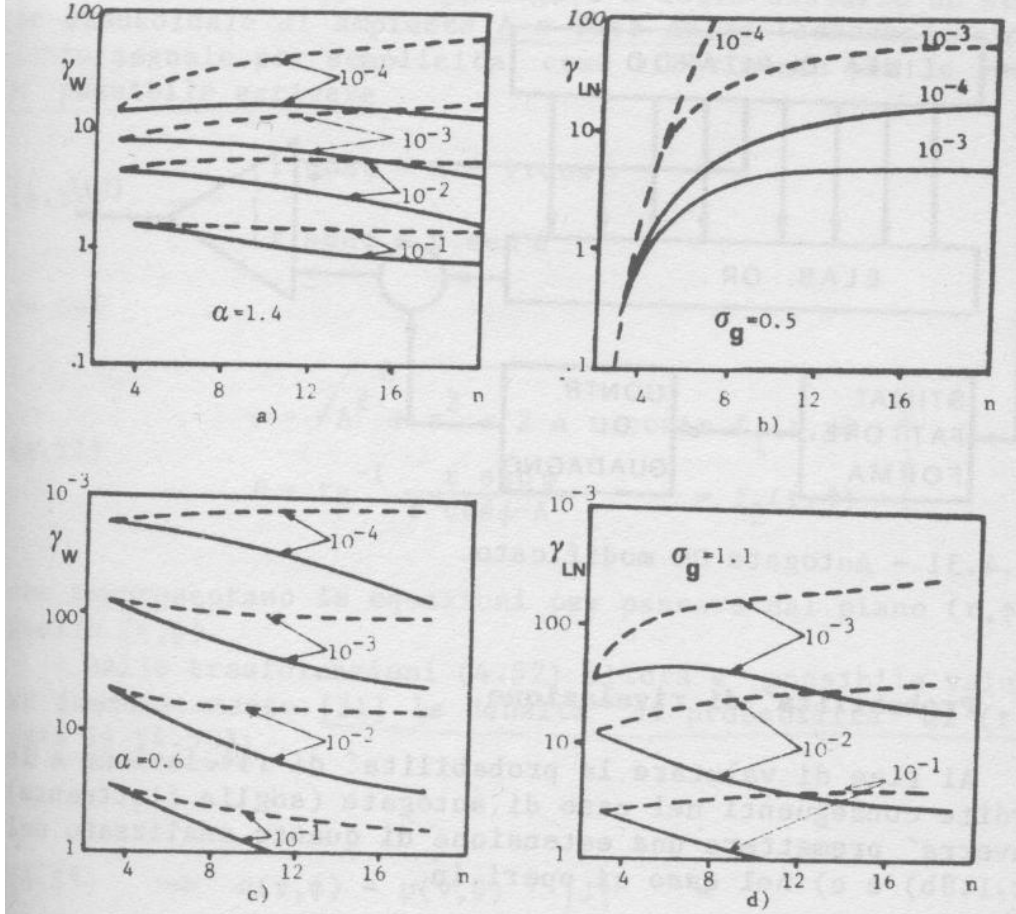

Fig.4.30 - Andamenti di γ per d.d.p. Weibull e Log-normali ed elaboratori AND ed OR.

From: G. Picardi "Elaborazione del segnale radar"

Impact of PDF on single pulse CFAR detection

- Unless appropriate detection schemes are used, the false alarm rate depends on the clutter spikiness

- **CFAR** against non-Gaussian clutter requires ad-hoc detection schemes that normalize out not only the mean power level, but also the spikiness of the distribution.

CFAR biparametrici (I)

Consider samples of K-distributed clutter:

EXAMPLE of NON-GAUSSIAN

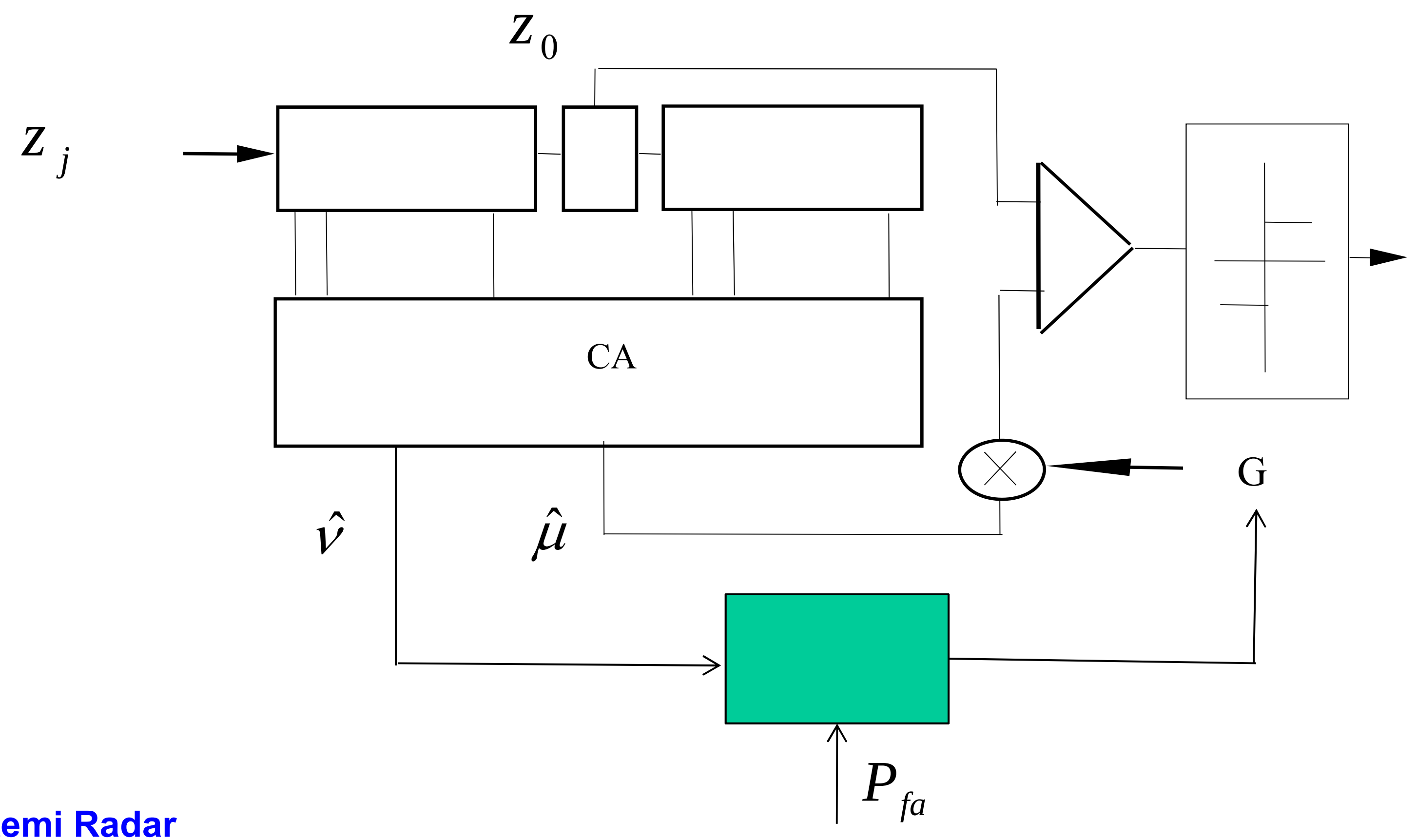

CFAR biparametrici (II)

Consider samples of Lognormal clutter:
EXAMPLE of NON-GAUSSIAN

$$p_x(x)=\frac{1}{\sqrt{2\pi\sigma x}}e^{-\frac{(\ln x-\ln m)^2}{2\sigma^2}} \qquad x>0$$

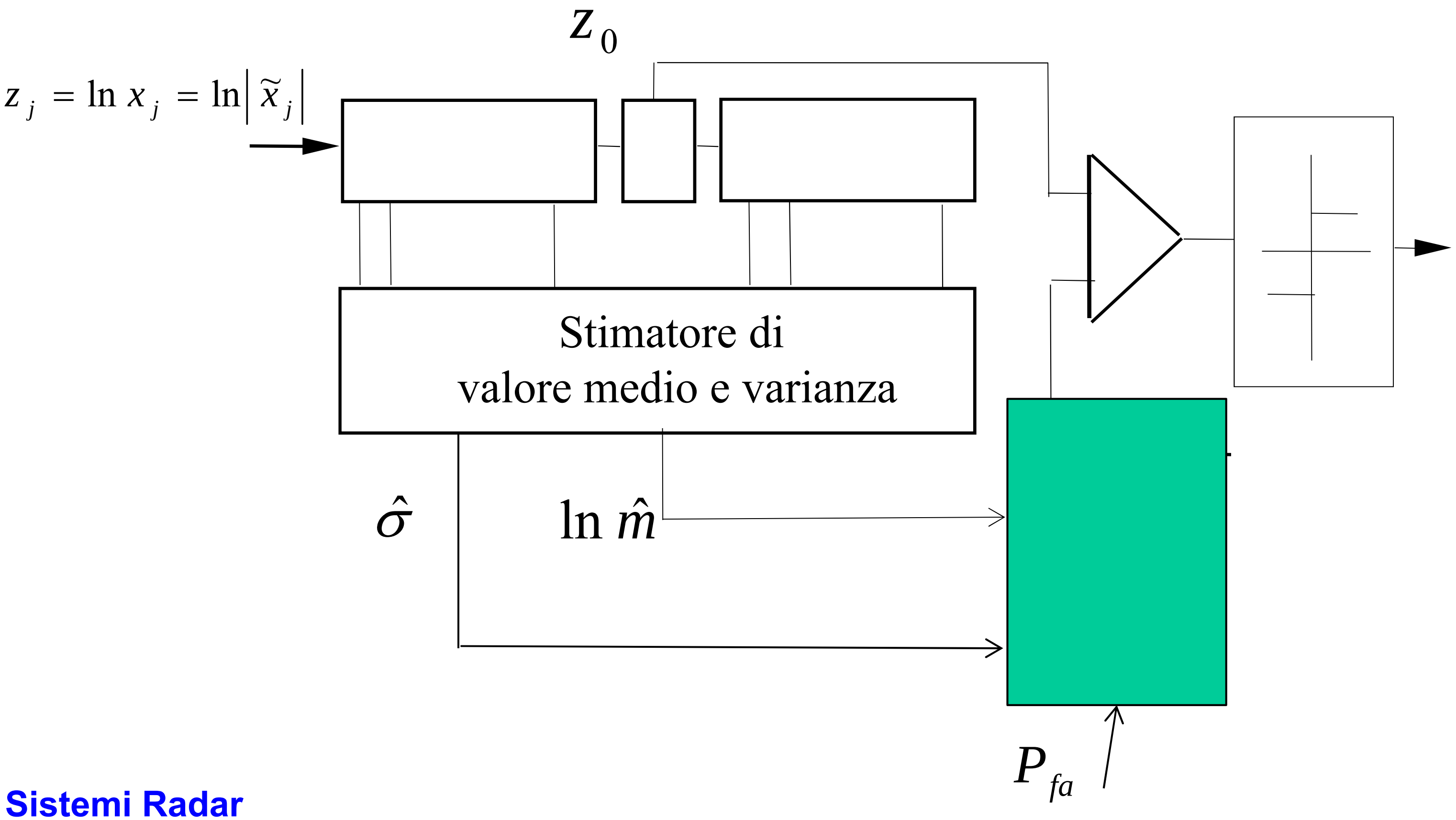

CFAR biparametrici (III)

Consider samples of Weibull clutter:

EXAMPLE of NON-GAUSSIAN

$$p_x(x)=\frac{\alpha}{\beta}\left(\frac{x}{\beta}\right)^{\alpha-1} e^{-\left(\frac{x}{\beta}\right)^{\alpha}} \qquad x\geq 0$$

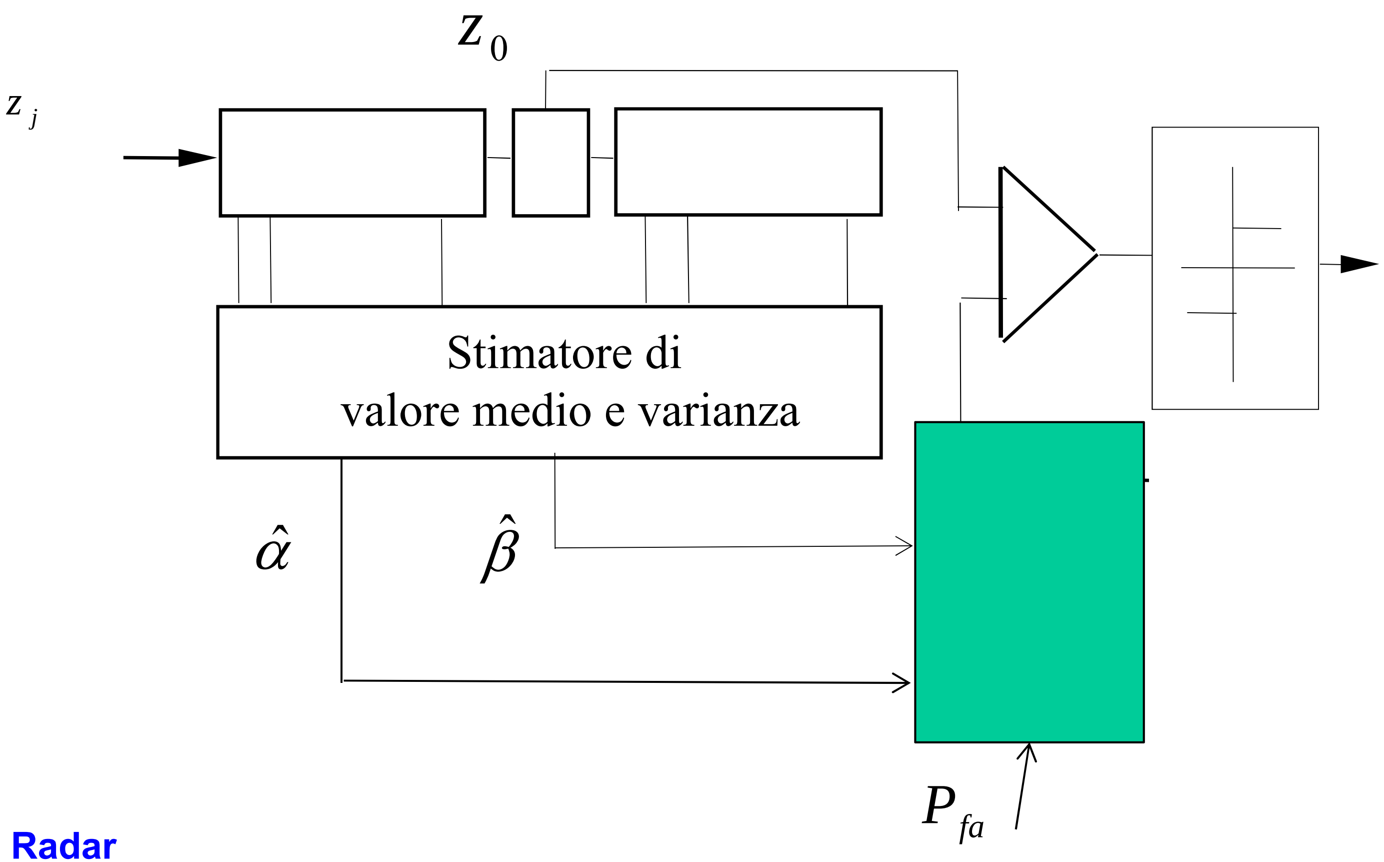

z_0

z_j

Stimatore di
valore medio e varianza

$\hat{\alpha}$

$\hat{\beta}$

P_{fa}

Clutter Map CFAR per NonGaussiano

- **Autogate:**

  - per clutter nongaussiano è “difficile” stimare due parametri da un numero limitato di celle in range (stime “poco accurate”). Aumentare le celle causa perdità di omogeneità ed estensione dei transitori.

- **Clutter map:** usa gli stessi schemi per la stima del livello di clutter, ma usando campioni della stessa cella in scan successivi:

  - per clutter nongaussiano “più semplice” stimare due parametri, specie usando anche alcune celle in range adiacenti, oltre l’informazione da scan a scan.